

ELECTRONIC APPENDIX

This is the Electronic Appendix to the article

Evolution of cooperation by generalized reciprocity

by

Thomas Pfeiffer, Claudia Rutte, Timothy Killingback, Michael Taborsky, and
Sebastian Bonhoeffer

Proc. R. Soc. B (doi:10.1098/rspb.2004.2988)

Electronic appendices are refereed with the text; however, no attempt is made
to impose a uniform editorial style on the electronic appendices.

Electronic Appendix

1. Evolution of strategies of direct reciprocity

To compare our simulation of generalized reciprocity (Fig 1 of the manuscript) with direct reciprocity we performed population dynamical simulations for group size 2. Because for group size 2, individuals interact repeatedly with the same partner, there is no difference between direct and generalized reciprocity. The methods used in our simulations are analogous to those described in the Appendix of the manuscript. To calculate the dynamic of interactions we use the transition matrix for the synchronous iPD in direct reciprocity (Nowak & Sigmund 1993; Nowak & Sigmund 1994). We use the same parameter set as for the simulations of generalized reciprocity. This implies that in comparison to previous publication on direct reciprocity we use a u-shaped distribution that is more biased towards extreme values and a larger initial frequency for new strategies. The simulations are repeated 100 times. The simulations are similar to those described previously (Nowak & Sigmund 1993; Nowak & Sigmund 1994). However, because of the large initial frequency of invading strategies, TFT is not the only strategy that can establish cooperation. PAVLOV emerges in 92% of the simulations, while GTFT emerges in 8% of the simulations. An example run is shown in Fig. 1 of the Electronic Appendix.

2. Agent-based simulations

To study the invasion of A-TFT and the evolution of anonymous strategies in finite, viscous populations with local reproduction we performed agent-based simulations for a group size of 2, 3, 5, and 10. The size of the population is 10,000 individuals for group size 2 (i.e., 5,000 groups), 5 (i.e., 2,000 groups) and 10 (i.e., 1,000 groups), and 9,999 individuals for group size 3 (i.e., 3,333 groups). Within their life, individuals interact on average in 10,000 PD's with random members of their group. The dispersal rate is equal to the death rate (on average once per 10,000 PD's), i.e. individuals change their group on average once in their life. Dispersal is simulated by choosing two random individuals from the population that swap their groups. Local reproduction and death are simulated by choosing two random individuals of the same group. One of the individuals reproduces, while the other individual dies. The probabilities for the individuals to replace the other individual are $f_1/(f_1+f_2)$, and $f_2/(f_1+f_2)$, respectively, where f_1 and f_2 are the fitness values of the individuals. Relations to other update rules have been discussed previously (Nowak et al., 2004). The fitness of an individual is given by its average

payoff in the iPD over its entire life. Individuals that never interacted in a PD have zero fitness.

Since in contrast to the population dynamical simulations shown in the manuscript we here assume that individuals have a finite number of interactions within their group, an additional probability p_I needs to be specified, that describes the probability of cooperation in the first move after birth or dispersal of an individual. This probability has only a small impact on fitness because erroneous moves are more frequent ($\varepsilon=10^{-3}$) than birth and dispersal. Strategies are characterized by 5 probabilities (p_B, p_R, p_S, p_T, p_P). A-TFT is described by (0.999, 0.999, 0.001, 0.999, 0.001), allC is described by (0.999, 0.999, 0.999, 0.999, 0.999), and allD is described by (0.001, 0.001, 0.001, 0.001, 0.001). We show three sets of simulations: (i) invasion of A-TFT in a population of allD; (ii) competition between allD, A-TFT, and allC; (iii) evolution of (real-valued) anonymous strategies. The frequency of mutation (from any strategy to any other) in simulations (i) and (ii) is 10^{-3} per reproduction event. Note that the mutation rate may have an impact on the simulation results since disadvantageous strategies fluctuate around a mutation-selection-equilibrium. In simulation set (iii) the overall mutation rate is 10^{-3} per reproduction event. New strategies are generated using the u-shaped distribution described in the Appendix of the manuscript. Note that only a small fraction of mutations result in A-TFT or similar strategies, which can drift into the population. Therefore, invasion may take longer compared to simulations (i) and (ii). Simulations for the payoff values (0, 1, 3, 4) are shown in Fig. 2 of the Electronic Appendix. Simulations for the payoff values (0, 1, 10, 11) are shown in Fig. 3 of the Electronic Appendix. Each simulation is replicated at least once. In contrast to the population dynamical simulations (Fig 1 of the manuscript and Fig 1 of the Electronic Appendix) we can simulate only a comparably low number of generations (2,000 for simulation set (i) and (ii), and 5,000 for simulation set (iii)). Therefore, the population dynamical simulations allow much better to study the long-term evolution of strategies.

Figure Legends for the Electronic Appendix.

Fig 1. Population dynamical simulation for the evolution of strategies of direct reciprocity. The methods used in the simulation are analogous to those used for the simulation of the evolution of generalized reciprocity (Fig. 1 of the manuscript). The figure shows the number of strategies in the population, the average payoff per individual per encounter, and the average probabilities (p_1 , p_2 , p_3 , p_4). We start with a population of unconditional defectors. TFT emerges in generation 2,000, resulting in an average payoff of 2 in the population. After TFT establishes cooperation it is replaced by a more generous strategy with values of about (1.0, 0.3, 0.8, 0.9). In the following phase of competition, PAVLOV emerges and dominates the population for the remaining time of the simulation. The dynamics of the evolution of direct reciprocity is similar to the evolution of generalized reciprocity (Fig. 1 of the manuscript).

Fig 2. Agent-based simulations the evolution of generalized reciprocity in a finite, viscous population with local reproduction. The payoff values are $S=0$, $P=1$, $R=3$, $T=4$. An average payoff in the population that is larger than the payoff for mutual defection ($P=1$) indicates the emergence of cooperation. Note that for group size 2, there is no difference between generalized and direct reciprocity. **(A-D)** Invasion of A-TFT into a population of unconditional defectors. The plots show the frequencies of the strategies allD, A-TFT, and allC, and the average payoff in the population. In groups of size 2, 3 and 5, A-TFT can emerge in the population, resulting in an average payoff of about $2=(P+R)/2$. If rare, A-TFT has only a small selective disadvantage in the non-cooperative population. Thus mutations from allD to A-TFT can accumulate such that A-TFT grows to a significant proportion of the population. If present at a sufficient frequency, A-TFT benefits from cooperative interactions in groups that consist exclusively of A-TFT players, and has a selective advantage over allD. Once A-TFT has taken over a population, allD cannot invade into the population since it has a large selective disadvantage. For group size 10, cooperation does not emerge in the simulation shown here. Although A-TFT may reach high levels in the population, the average payoff in the population stays close to $P=1$. Extensive simulations, however, indicate that even for the payoff values used here, A-TFT occasionally can take over the population. The emergence of cooperation by a successful invasion of A-TFT within the first 2,000 generations has been observed in 2 of 12 simulations. **(E-H)** For group size 2, 3, and 5, competition between allD, A-TFT, and allC leads to cycling between the three strategies. First, allD is invaded by A-

TFT. Once A-TFT has established cooperation, allC can invade the population and can replace A-TFT. allC, however, can be invaded by allD, resulting in oscillations between the three strategies. For group size 10, A-TFT and allC cannot emerge. **(I-L)** Evolution of strategies of generalized reciprocity. For group size 2, strategies close to A-PAVLOV emerge. In the simulations for group 3 and 5, A-GTFT is successful, indicating a trend from A-PAVLOV to A-GTFT with increasing group size. For group size 10, cooperation does not emerge, although the values of p_i , p_1 , and p_3 may drift to significant levels in the population. Note that because of the relatively low number of generations we cannot study the long term evolution of strategies as detailed as in the population dynamical simulations.

Fig 3. Agent-based simulations for the invasion of A-TFT into a finite, viscous population with local reproduction. The payoff values are $S=0$, $P=1$, $R=10$, $T=11$. **(A-D)** The simulations show that for low cost/benefit-ratio of cooperative behavior, A-TFT can emerge if individuals are interacting in groups with up to 10 individuals. As in Suppl. Fig. 2, the frequency of A-TFT initially increases due to mutations from allD. If present at a sufficient level, A-TFT can take over the population. **(E-H)** Competition between allD, BLIND TFT, and allC leads to oscillations between the strategies. **(I-L)** Evolution of strategies of generalized reciprocity. For group size 2 and 3, strategies close to A-PAVLOV emerge. In the simulations for group size 5, A-GTFT is successful. For group size 10, cooperation does not emerge within the first 5,000 generations. However, we observe short periods with a low degree of cooperation after generation 4,000. Note that compared to Fig 2 C and F, where cooperation does evolve for group size 10, the mutation rate to A-TFT is much lower, because only a small fraction of the mutations results in strategies such as A-TFT that can drift into the population.

Figure 1 (Electronic Appendix)

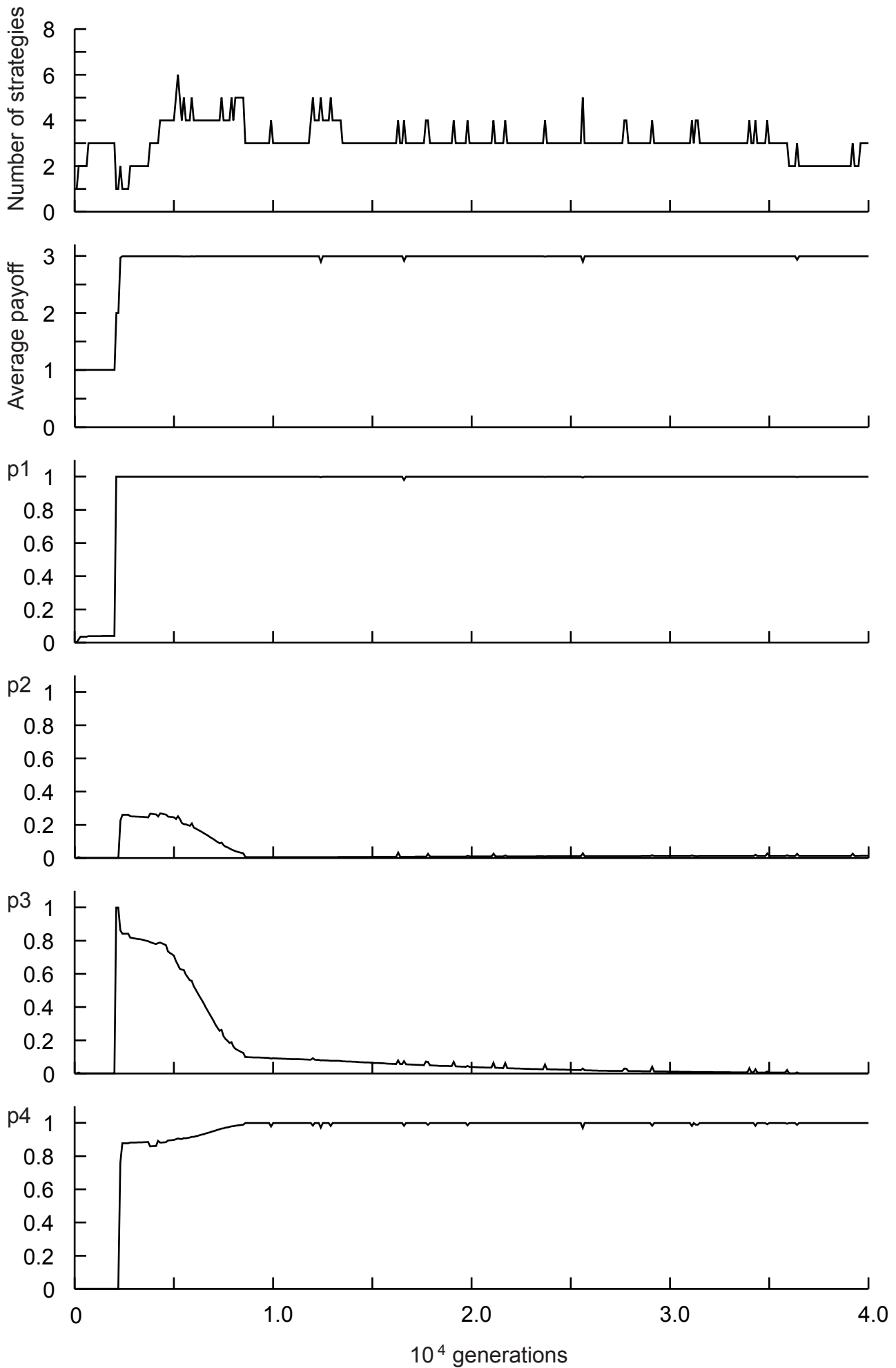
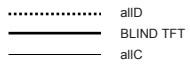


Figure 2 (Electronic Appendix)

Legend



Payoff values: S=0, P=1, R=3, T=4

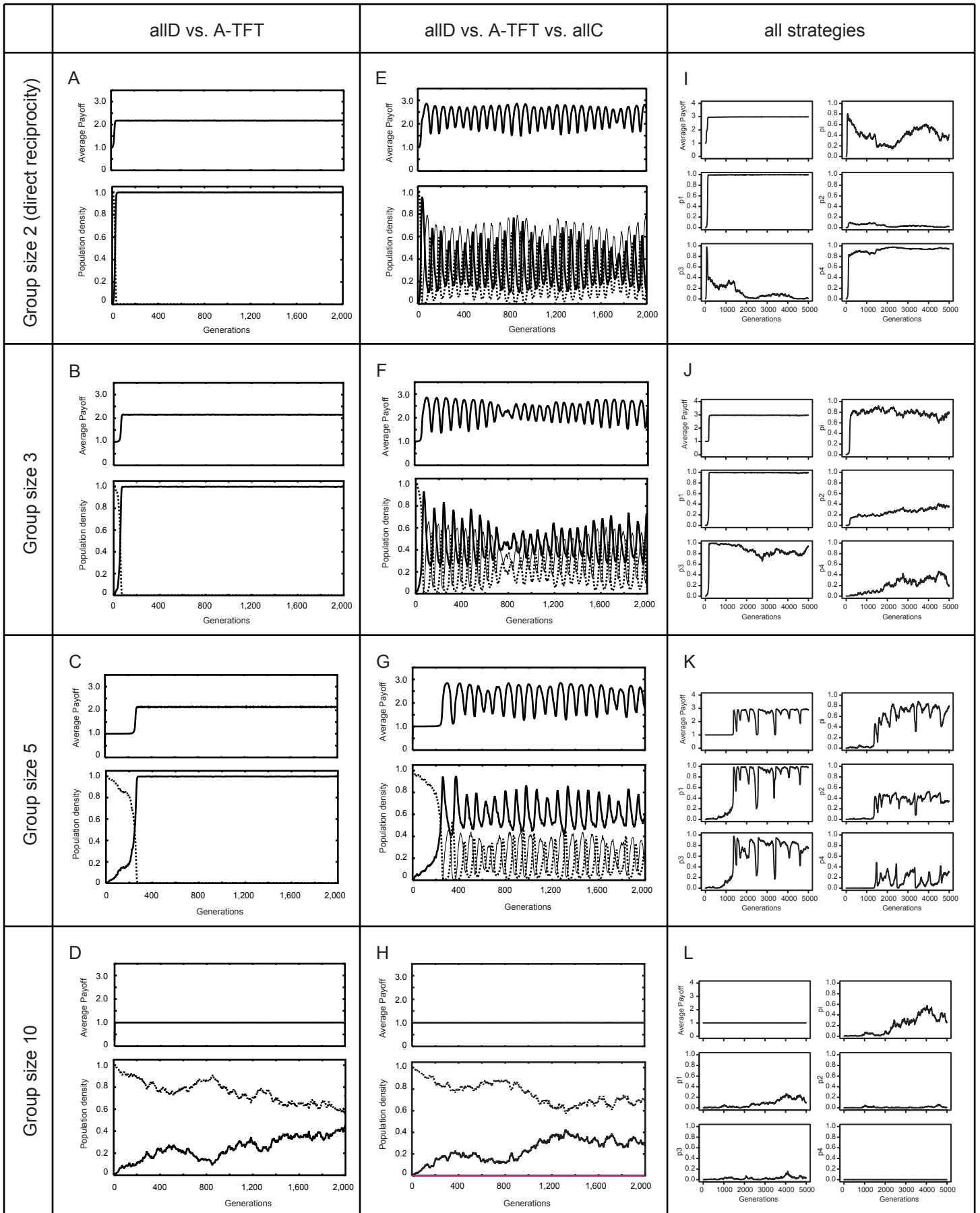


Figure 3 (Electronic Appendix)

Legend

- allD
- BLIND TFT
- allC

Payoff values: S=0, P=1, R=10, T=11

